Brain Research 1651 (2016) 88–94

Contents lists available at ScienceDirect

Brain Research

journal homepage: www.elsevier.com/locate/brainres

Altered glutamate release in the dorsal striatum of the MitoPark mouse model of Parkinson's disease

Ariana Q. Farrand [a], Rebecca A. Gregory [a,b], Cristina M. Bäckman [c], Kristi L. Helke [b], Heather A. Boger [a,*]

[a] Department of Neuroscience and Center on Aging, Medical University of South Carolina, 173 Ashley Ave, BSB 403, MSC 510, Charleston, SC 29425, USA
[b] Department of Comparative Medicine, Medical University of South Carolina, 114 Doughty St, STB 648, MSC 777, Charleston, SC 29425, USA
[c] Integrative Neuroscience Section, National Institute on Drug Abuse Intramural Research Program, National Institutes of Health, 251 Bayview Blvd, Baltimore, MD 21224, USA

ARTICLE INFO

Article history:
Received 1 June 2016
Received in revised form
12 September 2016
Accepted 18 September 2016
Available online 20 September 2016

Keywords:
In vivo electrochemistry
Glutamate
Striatum
Neurodegeneration
MitoPark
Dopamine

ABSTRACT

Mitochondrial dysfunction has been implicated in the degeneration of dopamine (DA) neurons in Parkinson's disease (PD). In addition, animal models of PD utilizing neurotoxins, such as 6-hydroxydopamine and 1-methyl-4-phenyl-1,2,3,6-tetrahydropyridine, have shown that these toxins disrupt mitochondrial respiration by targeting complex I of the electron transport chain, thereby impairing DA neurons in these models. A MitoPark mouse model was created to mimic the mitochondrial dysfunction observed in the DA system of PD patients. These mice display the same phenotypic characteristics as PD, including accelerated decline in motor function and DAergic systems with age. Previously, these mice have responded to L-Dopa treatment and develop L-Dopa induced dyskinesia (LID) as they age. A potential mechanism involved in the formation of LID is greater glutamate release into the dorsal striatum as a result of altered basal ganglia neurocircuitry due to reduced nigrostriatal DA neurotransmission. Therefore, the focus of this study was to assess various indicators of glutamate neurotransmission in the dorsal striatum of MitoPark mice at an age in which nigrostriatal DA has degenerated. At 28 weeks of age, MitoPark mice had, upon KCl stimulation, greater glutamate release in the dorsal striatum compared to control mice. In addition, uptake kinetics were slower in MitoPark mice. These findings were coupled with reduced expression of the glutamate re-uptake transporter, GLT-1, thus providing an environment suitable for glutamate excitotoxic events, leading to altered physiological function in these mice.

1. Introduction

Mitochondrial dysfunction has been implicated in the degeneration of substantia nigra dopamine (SN-DA) neurons, which leads to behavioral impairments and ultimately Parkinson's disease (PD; Greenamyre and Hastings; 2004). Toxin and genetic models traditionally used to mimic PD demonstrated altered mitochondrial function as well as generation of PD-related behaviors and pathology (Dawson et al., 2010; Duty and Jenner, 2011). Recently, to better understand the role of mitochondrial dysfunction on the degeneration of the SN-DA neurons, a genetic mouse model was created in which mitochondrial function was disrupted in SN-DA neurons by the knockout of the nuclear genome-encoded mitochondrial Tfam gene (Larsson et al., 1998). These mice, coined MitoPark mice, develop severe mitochondrial respiratory chain deficiencies in SN-DA neurons, which ultimately lead to the progressive degeneration, as well as the PD-associated behavioral deficits (Good et al., 2011).

The MitoPark mice mimic the progression of PD in humans, with adult onset and slow progression of neurological symptoms (Ekstrand et al., 2007). The mouse phenotype includes a uniform and progressive loss of DA afferents in areas of the basal ganglia., The nigrostriatal DAergic projections innervating the dorsal striatum are strongly affected, while the mesolimbic projections which innervate the ventral striatum are spared (Ekstrand et al., 2007; Galter et al., 2010). The DAergic loss observed in MitoPark mice occurs over weeks to months, a more physiological model than the time course of days which is seen in toxin-induced models of PD, thus allowing for better understanding of mechanisms involved with PD pathology and progression. Due to the slow progression of disease in these mice, they make for a better tool to understand treatment strategies for PD. For example, previous studies have demonstrated that MitoPark mice are responsive to L-Dopa therapy with a differential response depending on disease state (Galter et al., 2010; Gellhaar et al., 2015). In addition, Shan et al. (2015) demonstrated behavioral evidence of striatal neuroplasticity in

* Corresponding author.
E-mail address: boger@musc.edu (H.A. Boger).

http://dx.doi.org/10.1016/j.brainres.2016.09.025
0006-8993/

response to DAergic denervation, as well as in response to chronic L-Dopa therapy. Furthermore, it was determined that the extent of striatal DAergic denervation determines when motor complications develop with L-Dopa treatment (Shan et al., 2015). This study also supported the notion that delaying L-Dopa therapy until behavioral symptoms become more severe did not delay the development of L-Dopa induced dyskinesia (LID).

While the exact mechanism for the formation of LID is unknown, glutamate over-activity in the basal ganglia has been implicated (DeLong and Wichmann, 2015). Specifically, it is thought that maladaptive plasticity in the dorsal striatum involving faulty interaction between glutamate and DA inputs play a role (Calabresi et al., 2000; Picconi et al., 2012). This notion is further supported by studies showing that glutamate receptor antagonists alleviated LID (Paoletti et al., 2011; Nicoletti et al., 2011). MitoPark mice, which have been previously shown to develop LID, have increased mRNA expression of glutamate receptors in the dorsal striatum, which may be contributing to the formation of these behavioral abnormalities (Shan et al., 2015). Therefore, the current study was designed to assess glutamate release in the dorsal striatum of MitoPark mice, at an age in which LID was previously determined to be present (28 weeks; Shan et al., 2015). In addition, we also assessed various markers associated with the uptake and clearance of glutamate from the synaptic cleft to determine a potential mechanism by which glutamate may impact behavioral abnormalities.

2. Results

2.1. Effects of mitochondrial dysfunction on striatal TH-immunoreactivity

Due to a deletion of the Tfam gene in DA neurons, MitoPark mice demonstrate a slow, progressive loss of the nigrostriatal DA system, similar to what is seen in PD. In this study, we assessed the striatal DAergic innervation by analyzing striatal tyrosine hydroxylase-immunoreactivity (TH-ir) in MitoPark and control mice (Fig. 1). As can be seen in Fig. 1A vs. 1B, 28 week old MitoPark mice have significantly lower striatal TH-ir compared to control mice ($T_{(12)}=9.821$, $p<0.001$). These data indicate that MitoPark mice have reduction in the nigrostriatal DA pathway as a result of a disruption of mitochondrial function in DA neurons.

2.2. Altered glutamate kinetics in MitoPark mice

Other neurotransmitter systems, such as the glutamatergic

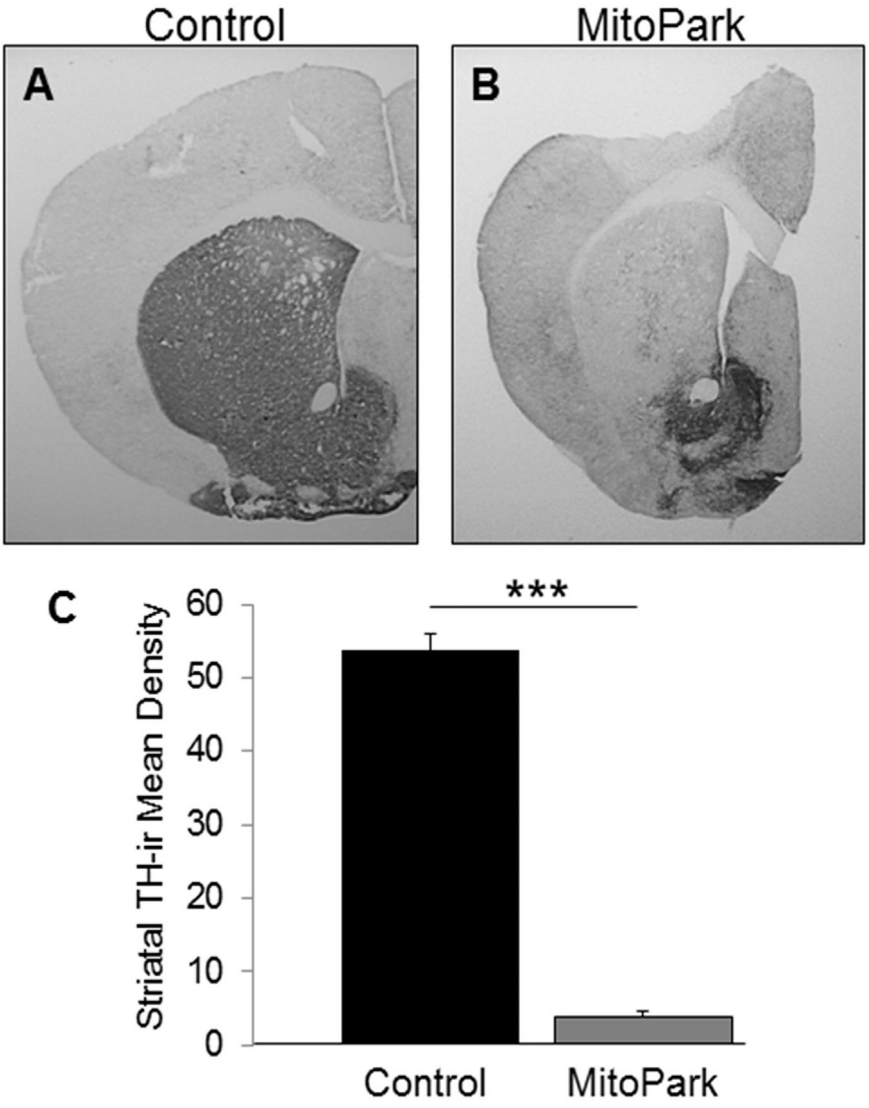

Fig. 1. Lower striatal TH-ir in MitoPark mice compared to controls. Photomicrographs (2x) of TH-ir in the dorsal striatum of (A) control and (B) MitoPark mice. (C) TH-ir is significantly lower in the dorsal striatum of MitoPark mice compared to control mice at 28 weeks of age (***$p<0.001$).

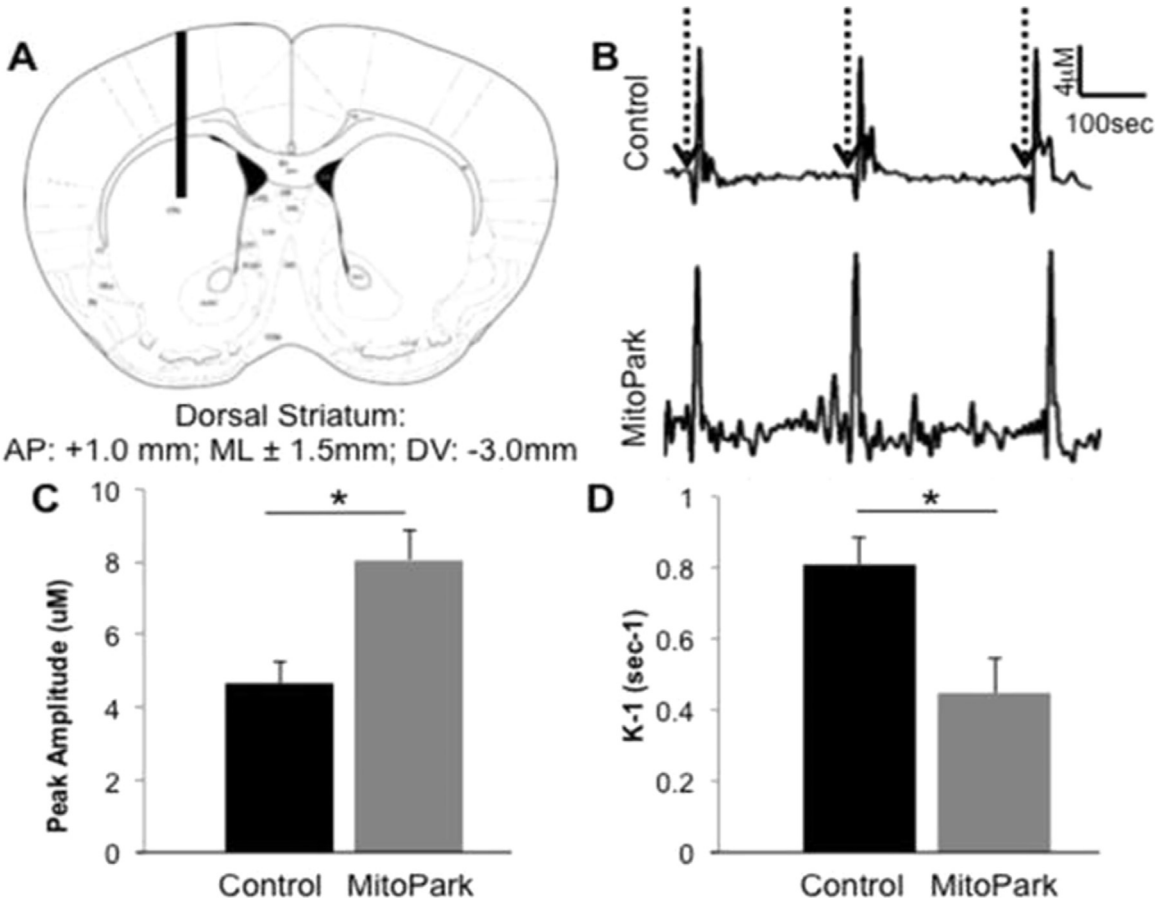

Fig. 2. Glutamate kinetics in the dorsal striatum of 28 week old MitoPark and control mice. (A) Microelectrode placement through the mouse dorsal striatum. The diagrams show the approximate location of the microelectrode at: AP+1.0 (relative to *bregma*; modified from Franklin and Paxinos (2001)). (B) Pressure ejection of 70 mM KCl (dotted arrows) caused release of glutamate in the dorsal striatum of control and MitoPark mice. (C) The amount of glutamate released in response to 70 mM KCl stimulation was greater in the dorsal striatum of MitoPark mice compared to age-matched control mice ($^*p < 0.05$). (D) Glutamate uptake was slower in MitoPark mice compared to age-matched control mice ($^*p < 0.05$).

system, play a role in the progression of DAergic degeneration (Blandini, 2010). In this study, we assessed striatal glutamate via in vivo electrochemistry to determine differences in transmission between 28 week old MitoPark and control mice (Fig. 2). Initially, we looked at KCl-stimulated glutamate release in the dorsal striatum of MitoPark mice at 28 weeks of age, an age previously shown to develop LID in these mice (Shan et al., 2015). Glutamate release was measured by the amplitude of the electrochemical peak produced in response to pressure ejected 70 mM KCl (Farrand et al., 2015) which was applied locally in the dorsal striatum (Fig. 2B (dotted arrows) and 2C). *T*-Test analysis revealed a significant increase in the amount of glutamate released in the dorsal striatum of MitoPark mice compared to control mice ($T_{(12)}=3.645$, $p < 0.05$). Additionally, we assessed the kinetics of glutamate uptake as it has been previously reported that excess glutamate in the synaptic cleft can result in excitotoxic events as a result of over-activation of post-synaptic receptors leading to cell death (Misonou et al., 2006). In this study we examined glutamate uptake by measuring k_{-1} (s^{-1}), a constant of the decay of glutamate clearance signals (Farrand et al., 2015). As can be seen in Fig. 2D, MitoPark mice had significantly slower glutamate clearance compared to control mice in the dorsal striatum ($T_{(12)}=5.903$, $p < 0.05$). These data together indicate that at 28 weeks of age, MitoPark mice have alterations in glutamate kinetics, which may affect neurotransmission and contribute to the formation of LID (Shan et al., 2015).

2.3. Effects of DAergic mitochondrial dysfunction on GLT-1 and GFAP expression in the dorsal striatum

The glutamate transporter, GLT-1, is predominantly located on astrocytes and is important for the uptake of glutamate from the extracellular space. Therefore, in this study, we wanted to assess the expression of GLT-1 in the dorsal striatum of MitoPark mice to determine its role in potential cell death mechanisms (Fig. 3A–C). As indicated, 28 week old MitoPark mice have significantly lower GLT-1-ir compared to control mice ($T_{(12)}=4.938$, $p < 0.01$). These data coupled with reduced glutamate uptake in the dorsal striatum of MitoPark mice indicate that dysfunction in glutamate clearance mechanisms can result in over-activation of postsynaptic neurons, which could result in behavioral abnormalities such as those that develop with the treatment of L-Dopa.

Astrogliosis is commonly associated with increased age, as well as with neurodegenerative diseases (Sofroniew, 2009); therefore, we wanted to assess GFAP expression in the dorsal striatum of MitoPark mice (Fig. 3D-F). *T*-test analysis determined that there is greater GFAP-ir in the dorsal striatum of MitoPark mice compared to controls ($T_{(12)}=4.929$, $p < 0.01$). These data confirm that the decrease in GLT-1 is not due to a decrease in astrocytes, as measured by GFAP-ir density, and also indicate that due to alterations in glutamate kinetics, coupled with a drastic reduction of nigrostriatal dopamine, MitoPark mice have greater GFAP expression occurring as a result of neurodegeneration.

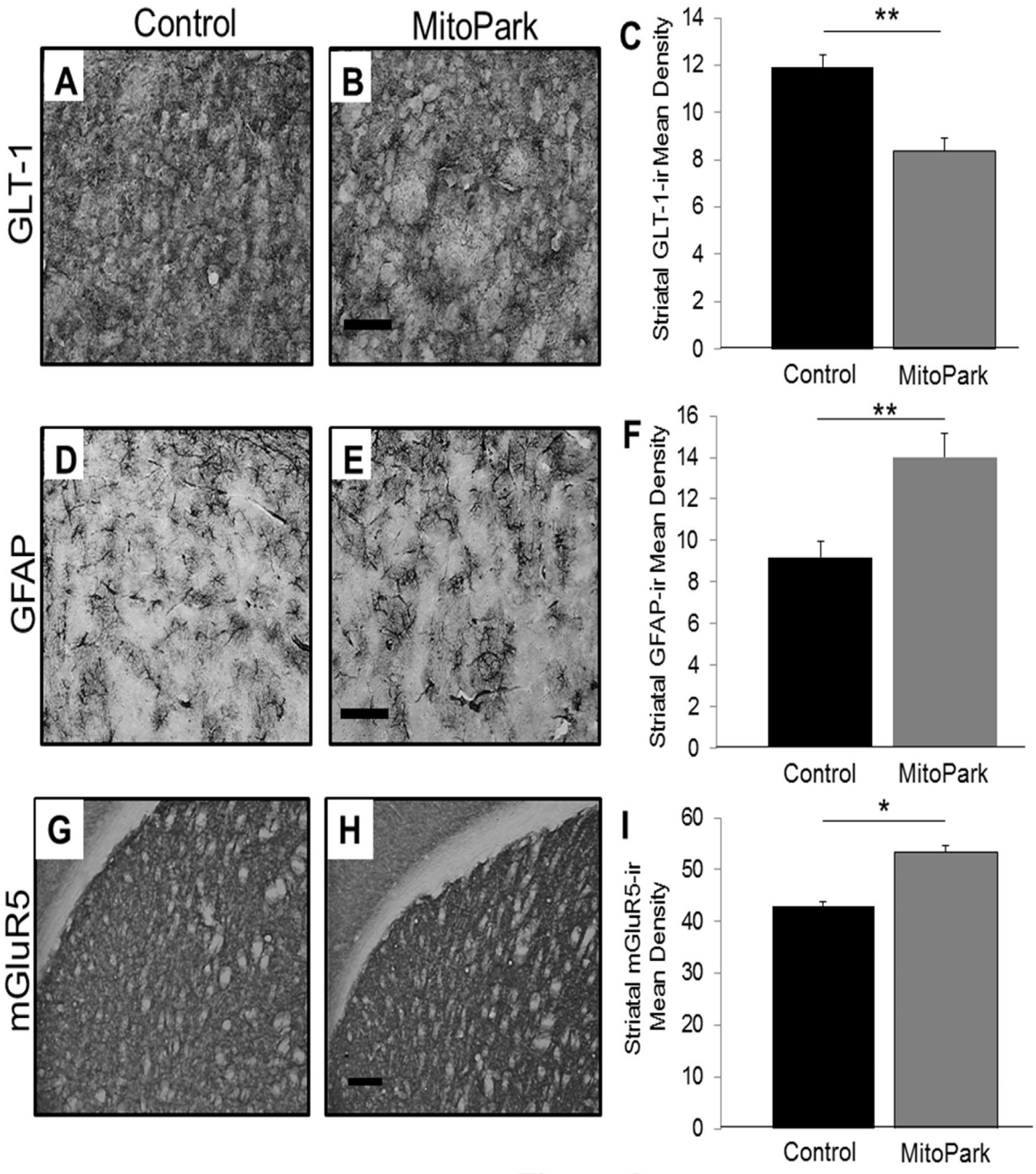

Fig. 3. Altered expression of GLT-1-ir, GFAP-ir, and mGluR5-ir in the dorsal striatum of MitoPark mice. Photomicrographs (60x) of GLT-1-ir in the dorsal striatum of (A) control and (B) MitoPark mice. (C) At 28 weeks of age, MitoPark mice had significantly lower GLT-1-ir in the dorsal striatum as compared to control mice (**$p < 0.01$). Scale bar = 0.5 mm. Photomicrographs (60x) of GFAP-ir in the dorsal striatum of (D) control and (E) MitoPark mice. (F) The dorsal striatum of MitoPark mice has significantly greater GFAP-ir compared to age-matched control mice (**$p < 0.01$). Scale bar = 0.5 mm. Photomicrographs (10x) of mGluR5-ir in the dorsal striatum of (G) control and (H) MitoPark mice at 28 weeks of age. (I) mGluR5-ir is significantly greater in the dorsal striatum of MitoPark mice compared to age-matched controls (*$p < 0.05$). Scale bar = 200 μm.

2.4. Differential mGluR5 expression in the dorsal striatum of MitoPark mice

The glutamate metabotropic receptor, mGluR5, is a predominantly post-synaptic receptor and is highly expressed within the basal ganglia (Paquet and Smith, 2003). Excess glutamate within the synaptic cleft can result in over-activation of the post-synaptic mGluR5 receptors, which leads to neuronal excitotoxicity (Misonou et al., 2006). Due to the alterations in glutamate release in MitoPark mice and based on previous data suggesting increased mRNA of mGluR5 receptor expression (Shan et al., 2015), we assessed mGluR5 expression via immunohistochemical detection in the dorsal striatum of 28 week old MitoPark and control mice (Fig. 3G–I). *T*-test comparison between the two genotypes demonstrate significantly higher mGluR5-ir in the dorsal striatum of MitoPark mice compared to control mice ($T_{(12)} = 12.734$, $p < 0.05$). These data coupled with the increased KCl-stimulated glutamate release in the dorsal striatum of MitoPark mice suggest a mechanism for increased post-synaptic receptor activation as a result of greater synaptic availability of glutamate.

3. Discussion

Results from these studies indicate that MitoPark mice have alterations in glutamate kinetics that may aid in the formation of LID

and further the degeneration of the nigrostriatal DA system (Ekstrand et al., 2007; Good et al., 2011; Shan et al., 2015). Our data indicate that at 28 weeks of age, MitoPark mice have greater KCl-stimulated glutamate release and higher mGluR5-ir. These findings are coupled with slower glutamate uptake and reduced GLT-1 expression in the dorsal striatum. These alterations in glutamate physiology coupled with the progressive loss of the nigrostriatal DA system result in an increase of GFAP expression within the dorsal striatum.

While previous studies have demonstrated an increased age-dependent degeneration of DA neurons in MitoPark mice, they also develop LID, similar to what is observed in PD. However, the exact mechanism for how treatment with L-Dopa results in dyskinetic behavior is unknown. A potential mechanism is the over-activation of glutamatergic systems within the basal ganglia. The overactivation of glutamatergic systems includes increased glutamate release into the synaptic cleft and reduced glutamate clearance from the cleft, both of which can ultimately result in greater binding to postsynaptic glutamate receptors, such as the mGluR5 on the medium spiny neurons in the dorsal striatum. The constant or over-activation of postsynaptic glutamate receptors can lead to greater cellular activity and increased Ca^{2+} influx which can ultimately contribute to cell death (Picconi et al., 2012).

In this study, we have demonstrated that when glutamate neurons are stimulated with 70 mM KCl, there is greater release in the dorsal striatum of MitoPark mice compared to control mice. This finding is consistent with previous studies that have demonstrated that when the nigrostriatal DA system is reduced or degenerating, the basal ganglia pathway becomes dysregulated which can ultimately lead to greater cortical glutamate release into the dorsal striatum (Tata and Yamamoto, 2008).

While some DAergic neurons also release glutamate, the primary source of glutamate input into the dorsal striatum is from cortical sources. Disruption of cortico-striatal connections has been shown to be involved in other motor disorders such as Huntington's disease (Dogan et al., 2015), and cortical involvement in the basal ganglia circuitry is likely at play in this model of PD, as well. Degeneration of SN-DA neurons ultimately decreases output of the basal ganglia, and it is likely that the increased glutamate release observed in this study is a downstream compensatory attempt by the corticostriatal system to balance activity of the basal ganglia. This claim is supported by other studies that have observed similar trends within both the basal ganglia and cortex after administration of 6-hydroxydopamine (Qiu et al., 2014), and the excitotoxic nature of the increased glutamate may also exacerbate the DAergic terminal degeneration that is already occurring in these areas.

Not only can increased glutamate release result in over-activation of post-synaptic glutamate receptors, but also the reduction of mechanisms to clear glutamate from the synaptic cleft can result in increased receptor binding and activation (Fischer et al., 2013). In the current study, we demonstrated that 28 week old MitoPark mice have reduced clearance/uptake of glutamate from the synaptic cleft in the dorsal striatum compared to control mice. This data was coupled with reduced expression of the glutamate transporter, GLT-1, which is predominantly expressed in astrocytes and is responsible for taking glutamate up to be processed and recycled by neurons (Armstrong et al., 2004; Scofield and Kalivas, 2014; Williams et al., 2005).

The observed reduction in GLT-1-ir expression in combination with the observed increase in GFAP-ir indicates that the reduced clearance from the synaptic cleft is due, at least in part, to a reduction in GLT-1 expression as opposed to an alteration of GLT-1 function. Previous studies have shown that astrogliosis is commonly associated with neurodegenerative diseases, and that these changes also alter the genetic expression of astrocytes (Sofroniew, 2009). Our data show that one of these genetic alterations is a reduction in GLT-1 expression. Further characterization of these genetic changes should be confirmed via measurements of messenger RNA and uptake assays.

As mentioned previously, greater levels of extracellular glutamate can result in over-activation of post-synaptic glutamate receptors, such as NMDARs and mGluRs. It is the overactivation of these classes of glutamate receptors that are thought to play a role in PD-related pathology, as well as the formation of LID (DeLong and Wichmann, 2015). Previous studies have shown that while MitoPark mice will respond behaviorally to L-Dopa initially, they will develop LID over time. Furthermore, it has been demonstrated that delaying the administration of L-Dopa does not delay the onset of the dyskinetic behavior in MitoPark mice (Ekstrand et al., 2007; Shan et al., 2015). In the latter study, the authors further indicated that the progressive loss of the nigrostriatal DA system gave rise to altered mRNA expression patterns for DAergic, GABAergic, cholinergic, serotonergic, and glutamatergic receptors in the dorsal striatum of MitoPark mice. Of interest to our current study was the increased mRNA expression of mGluR5 in MitoPark mice. Our study demonstrated that MitoPark mice do have greater mGluR5 levels as indicated by immunohistochemistry. Therefore, it is possible that the LID development published by others is regulated by this increased expression of the mGluR5 receptor, leading to greater neuronal activation within the dorsal striatum. This seems plausible since studies have shown that the administration of glutamate receptor antagonists, including the mGluR5 antagonist MPEP, have inhibited the onset of LID (Niswender and Conn, 2010; Gasparini et al., 2013; Rascol et al., 2014). Future studies should be conducted to truly elucidate the mechanism by which the increased glutamate release and decreased clearance is playing a role in the formation of dyskinetic behavior in MitoPark mice. These studies should include a full characterization of altered glutamate receptor expressions as well as the downstream signaling cascades that may contribute to LID formation.

4. Conclusions

Taken together, these data demonstrate that MitoPark mice have greater glutamate release, reduced glutamate uptake, and increased mGluR5 expression, all of which may lead to excitotoxicity. Future studies will be conducted to determine at what age glutamate release and uptake are altered in MitoPark mice and if the co-administration of a glutamate receptor antagonist in combination with L-Dopa will inhibit or reduce the formation of dyskinetic behavior.

5. Materials and methods

5.1. Animals

For these experiments, 28 week old male MitoPark mice were compared to control littermates (N = 6–7 per genotype). In order to create this mouse line, the Tfam loxP (Ekstrand et al., 2007) line was crossed with the B6.129(Cg)-*Slc6a3tm1(cre)Xz*/J (DAT-cre, Backman et al., 2006) to create a MitoPark colony at the Medical University of South Carolina, under National Institutes of Health (NIH)- and Institutional Animal Care and Use Committee-approved protocols. The Slc6a3 gene encodes Dopamine Transporter 1. Animals were genotyped using primers and PCR protocols published previously (Backman et al., 2006; Ekstrand et al., 2007) and utilizing the Extract-n-Amp Tissue Kit (Sigma). Experimental mice were homozygous for loxP insertion at the Tfam gene and heterozygous for DAT-cre expression (DAT/DATcre TfamloxP/TfamloxP). Control mice were littermates that had no DAT-cre expression and were either wildtype or heterozygous for loxP-flanking at the Tfam locus (DAT/DAT Tfam/Tfam or DAT/DAT Tfam/TfamloxP). The mice were housed three to five animals per cage with a

twelve-hour (hr) light/dark cycle. The room was kept at 20–22 °C, and food and water were provided ad libitum.

5.1.1. Enzyme-Based Glutamate Biosensor

S2 ceramic-based microelectrode arrays (MEA) were prepared for in vivo recordings as previously described (Burmeister et al., 2002; Quintero et al., 2011). Briefly, recording sites were coated with a glutamate oxidase (GluOx) enzyme solution (U.S. Biological) containing a final concentration of 1% bovine serum albumin (BSA, Sigma-Aldrich), 0.125% glutaraldehyde (Sigma-Aldrich), and 1% GluOx. After a 24-hr drying period, platinum sites were electroplated with an m-Phenylenediamine dihydrochloride size exclusion layer (Acros Organics) to block potential interfering analytes such as ascorbic acid (AA), catecholamines, and indoleamines (Burmeister et al., 2002; Hascup et al., 2008). The GluOx enzyme is required for measurement of glutamate as it metabolizes glutamate to α-ketoglutarate, which is then converted to the reporter molecule hydrogen peroxide (H_2O_2). When a potential of +0.7 V versus a silver/silver chloride reference electrode was applied to the MEA, H_2O_2 is oxidized resulting in the transfer of two electrons to the platinum recording surface. The resulting change in current was amplified and digitized by a FAST16 MKIII recording system (Quanteon, LLC).

5.1.2. Electrode calibration

MEAs were calibrated to determine their sensitivity to glutamate and selectivity against AA using constant potential amperometry with a FAST16 MKIII system as described previously (Burmeister et al., 2002; Quintero et al., 2011). Briefly, the MEA was submerged in 40 mL of a continuously stirred solution of 0.05 M phosphate-buffered saline filtered and titrated to pH 7.4 and allowed to reach a stable baseline for ~60 min before calibrating. Phosphate buffer temperature was maintained at 37 °C using a circulating water bath (Gaymar Industries). Aliquots of freshly made 20 mM AA and 20 mM glutamate were used to obtain final concentrations of 250 μM AA and 20, 40, and 60 μM glutamate for all calibrations. Selectivity ratios for glutamate over AA were calculated in addition to the limit of detection (LOD) and linearity (R^2) for all glutamate MEAs. Reported as mean ± S.E.M., the MEAs had average selectivity ratios of 35 ± 13: 1, LOD of 0.8 ± 0.4 μM and R^2 values of 0.998 ± 0.002. The MEAs were also tested to compare the recording capability among the platinum recording sites using H_2O_2 (8.8 μM, final concentration) as a test substance. Electrodes that did not respond to H_2O_2, had R^2 values < 0.99, or had LODs > 5 μM were excluded. After calibration, MEAs were fitted with single-barrel glass capillaries that were pulled and bumped to an inner tip diameter of approximately 10 μm. The pipette was attached under a dissection scope in order to place the tip of the pipette above the glutamate sensitive sites, 75 μm from the surface of the MEA (Burmeister et al., 2002; Smith et al., 2007). The pipette was filled with freshly made KCl solution containing 70 mM KCl, 79 mM NaCl, and 2.5 mM $CaCl_2$ at pH 7.4, attached to the headstage, and connected to a Picospritzer III (Parker Instruments).

5.1.3. In vivo glutamate electrochemistry

The electrode was implanted into the mouse dorsal striatum based on previously established protocols (ie. Hoffman and Gerhardt, 1998). Mice were anesthetized with 12.5% urethane at 0.01 mL/g body weight injection volume and placed in a stereotaxic apparatus (David Kopf Instruments) fitted with a 37 °C heating pad. Following removal of the scalp tissue, mice underwent a craniotomy, leaving bregma intact. Mice were implanted with a glutamate-selective MEA-KCl pipette assembly into the left and right striatum (AP, +1.0 mm; mL, ±1.5 mm; DV, −3.0 mm relative to bregma; Franklin and Paxinos, 2001; Fig. 2A). A small hole was drilled at the back of the skull above the parietal cortex for placement of the silver/silver chloride reference electrode. Once the MEA was lowered, mice underwent a minimum of 30 min acclimation period to allow the electrode to equilibrate at the target depth after breaking through cortical tissue to reach the striatum and to establish a stable baseline recording. Following baseline period, pressure ejections of 70 mM KCl solution were performed using the Picospritzer III microinjection dispensing system. Pressure ejection of 70 mM KCl (70 mM KCl, 79 mM NaCl, 2.5 mM $CaCl_2$, pH 7.4) has been repeatedly shown to lead to a depolarization event and release of glutamate into the extra-cellular space, causing a robust and reproducible rise in the glutamate signal compared to baseline (Hascup et al., 2007, 2012; Farrand et al., 2015). The maximum change in concentration compared to baseline is referred to as maximum amplitude or amplitude of the glutamate signal. This value is normally recorded in μM units. Approximately 150 nL of KCl solution was pressure ejected adjacent to the microelectrode to induce depolarization and subsequent release of glutamate into the striatum. KCl ejection resulted in reproducible glutamate peaks detected by MEAs (Fig. 2B; dotted arrows denote pressure ejection of KCl). Following each KCl ejection, recordings were allowed to return to baseline for at least 100 s before repeating the procedure. This procedure was repeated 6–8 times for each recording site.

5.1.4. Electrochemistry data analysis

The FAST16 MKIII recording system saved amperometric data, time, and experimenter mediated ejection marks. All data traces from MEAs were analyzed with the FAST Analysis software (Jason Burmeister Consulting, LLC), a program written and compiled in Matlab from Mathworks. As previously published (Hebert et al., 1996; Day et al., 2006; Farrand et al., 2015), the FAST Analysis software was used to determine peak amplitude (pressure ejected 70 mM KCl-evoked glutamate release, μM) and k_{-1} (glutamate uptake, s^{-1}). All data were passed through a low stringency wavelet low pass filter (using the Daubechies wavelet) to remove high frequency noise.

5.2. Brain preparation

Upon completion of electrochemical recordings, the mice were decapitated while deeply anesthetized. The left and right rostral portion of the brain containing the dorsal striatum was blocked and placed in 4% paraformaldehyde at 4 °C. After 48 h, the tissue block was placed in 30% sucrose for at least 24 h before cryo-sectioning for immunohistochemistry (45 μm; Microm). Section thickness was chosen according to our established protocols for conducting free-floating immunohistochemistry (Boger et al., 2006; Farrand et al., 2015).

5.3. Immunohistochemical staining

Immunohistochemistry in the dorsal striatum was performed on free-floating serial sections (every 6th section) using a rabbit polyclonal tyrosine hydroxylase antibody (TH; 1:1000 Pelfreez), a rabbit polyclonal glial fibrillary acidic protein antibody (GFAP; 1:2000 Dako), a rabbit polyclonal glutamate transporter 1 (GLT-1; 1:1000 Abcam), or a rabbit polyclonal metabotropic glutamate receptor 5 antibody (mGluR5; 1:2000 Millipore). Briefly, primary antibodies were applied to free-floating serial sections taken every 6th section from the dorsal striatum based on our previous protocols (Boger et al., 2006; Farrand et al., 2015). Endogenous peroxidase activity was quenched by treating sections with 10% H_2O_2 in 20% methanol for 10 min. Sections were then permeabilized in TBST (TBS with 0.25% TritonX-100) following treatment for 20 min with sodium meta-periodate. Non-specific binding was controlled by incubation in 10% normal goat serum (NGS) for 1 h. Sections were then incubated overnight in the primary antibody at room temperature. The next day, sections were incubated for 1 h with the secondary antibody (1:200; biotinylated goat anti-rabbit serum Vector Laboratories) and 1 h with avidin-biotin complex (ABC kit,

Vector labs). The reaction was developed using VIP peroxidase substrate kit (Vector labs) to enhance the reaction and produce a dark color stain. This reaction was stopped using 0.01 M TBS, and the sections were mounted on glass slides, dehydrated, and coverslipped with DPX (Sigma). To determine antibody specificity, we also conduct immunohistochemistry in which a subset of sections is processed with no primary antibody and a subset of sections processed with no secondary antibody. As seen in Supplemental Fig. 1, these sections demonstrate no staining in the absence of either the primary or secondary antibody for each marker used in this study.

5.4. Semiquantitation of dorsal striatum Immunostaining

Staining intensity of TH, GFAP, GLT-1, and mGluR5 in the dorsal striatum, was determined using NIH Image J Software to measure a gray scale value within the range of 0–256, where 0 represents white and 256 black. A template for the dorsal striatum was created and used on all brains similarly, and images were captured with a Nikon Eclipse E-600 microscope using the 10× objective, or an Olympus-750 video camera system, and a Dell Pentium III computer. Measurements were performed blinded and included the dorsal striatum bounded on the superior and lateral sides by the curve of the corpus callosum and medially by the lateral ventricle and excluding the ventral striatum. Measurements from 5 sections were averaged to obtain one value per subject. Staining density was obtained when background staining was subtracted from mean staining intensities on every 6th section through the dorsal striatum for all four antibodies.

5.5. Statistical analysis

Electrochemical and immunohistochemical data were analyzed utilizing Student's *T*-test analysis using Statview. Significance is reported as $p < 0.05$.

Acknowledgments

Funding: This work was supported by the MUSC Barmore Fund, Charleston, SC and the National Institute on Aging at the National Institutes of Health (Grant 4R00AG033687).

Appendix A. Transparency document

Transparency document associated with this article can be found in the online version at http://dx.doi.org/10.1016/j.brainres.2016.09.025.

References

Armstrong, V., et al., 2004. Repeated amphetamine treatment causes a persistent elevation of glial fibrillary acidic protein in the caudate-putamen. Eur. J. Pharm. 488, 111–115.
Blandini, F., 2010. An update on the potential role of excitotoxicity in the pathogenesis of Parkinson's disease. Funct. Neurol. 25, 65–71.
Boger, H.A., et al., 2006. A partial GDNF depletion leads to earlier age-related deterioration of motor function and tyrosine hydroxylase expression in the substantia nigra. Exp. Neurol. 202, 336–347.
Burmeister, J.J., et al., 2002. Improved ceramic-based multisite microelectrode for rapid measurements of L-glutamate in the CNS. J. Neurosci. Methods 119, 163–171.
Bäckman, C.M., et al., 2006. Characterization of a mouse strain expressing Cre recombinase from the 3′ untranslated region of the dopamine transporter locus. Genesis 44, 383–390.
Calabresi, P., et al., 2000. Levodopa-induced dyskinesia: a pathological form of striatal synaptic plasticity? Ann. Neurol. 47, S60–S68 (discussion S68-9).
Dawson, T.M., et al., 2010. Genetic animal models of Parkinson's disease. Neuron 66, 646–661.
Day, B.K., et al., 2006. Microelectrode array studies of basal and potassium-evoked release of L-glutamate in the anesthetized rat brain. J. Neurochem. 96, 1626–1635.
DeLong, M.R., Wichmann, T., 2015. Basal ganglia circuits as targets for neuromodulation in Parkinson disease. JAMA Neurol. 72, 1354–1360.
Dogan, I., et al., 2015. Functional connectivity modeling of consistent cortico-striatal degeneration in Huntington's disease. Neuroimage Clin. 7, 640–652.
Duty, S., Jenner, P., 2011. Animal models of Parkinson's disease: a source of novel treatments and clues to the cause of the disease. Br. J. Pharmacol. 164, 1357–1391.
Ekstrand, M.I., et al., 2007. Progressive parkinsonism in mice with respiratory-chain-deficient dopamine neurons. Proc. Natl. Acad. Sci. USA 104, 1325–1330.
Farrand, A.Q., et al., 2015. Effects of aging on glutamate neurotransmission in the substantia nigra of Gdnf heterozygous mice. Neurobiol. Aging 36, 1569–1576.
Fischer, K.D., et al., 2013. Role of the major glutamate transporter GLT1 in nucleus accumbens core versus shell in cue-induced cocaine-seeking behavior. J. Neurosci. 33, 9319–9327.
Franklin, K.B.J., Paxinos, G., 2001. The Mouse Brain in Stereotaxic Coordinates. Academic Press, San Diego, CA.
Galter, D., et al., 2010. MitoPark mice mirror the slow progression of key symptoms and L-DOPA response in Parkinson's disease. Genes Brain Behav. 9, 173–181.
Gasparini, F., et al., 2013. Metabotropic glutamate receptors for Parkinson's disease therapy. Park. Dis. 2013, 196028.
Gellhaar, S., et al., 2015. Chronic L-DOPA induces hyperactivity, normalization of gait and dyskinetic behavior in MitoPark mice. Genes Brain Behav. 14, 260–270.
Good, C.H., et al., 2011. Impaired nigrostriatal function precedes behavioral deficits in a genetic mitochondrial model of Parkinson's disease. FASEB J. 25, 1333–1344.
Greenamyre, J.T., Hastings, T.G., 2004. Biomedicine. Parkinson's–divergent causes, convergent mechanisms. Science 304, 1120–1122.
Hascup, K.N., et al., 2007. Second-by-Second Measures of L-Glutamate and Other Neurotransmitters Using Enzyme-based Microelectrode Arrays, Electrochemical Methods for Neuroscience. CRC Press, Boca Raton, FL (Chapter 19).
Hascup, K.N., et al., 2008. Second-by-second measures of L-glutamate in the prefrontal cortex and striatum of freely moving mice. J. Pharm. Exp. Ther. 324, 725–731.
Hascup, E.R., et al., 2012. An allosteric modulator of metabotropic glutamate receptors ($mGluR_2$), (+)-TFMPIP, inhibits restraint stress-induced phasic glutamate release in rat prefrontal cortex. J. Neurochem. 122, 619–627.
Hebert, M.A., et al., 1996. Functional effects of GDNF in normal rat striatum: presynaptic studies using in vivo electrochemistry and microdialysis. J. Pharm. Exp. Ther. 279, 1181–1190.
Hoffman, A.F., Gerhardt, G.A., 1998. In vivo electrochemical studies of dopamine clearance in the rat substantia nigra: effects of locally applied uptake inhibitors and unilateral 6-hydroxydopamine lesions. J. Neurochem 70, 179–189.
Larsson, N.G., et al., 1998. Mitochondrial transcription factor A is necessary for mtDNA maintenance and embryogenesis in mice. Nat. Genet. 18, 231–236.
Misonou, Y., et al., 2006. Acrolein produces nitric oxide through the elevation of intracellular calcium levels to induce apoptosis in human umbilical vein endothelial cells: implications for smoke angiopathy. Nitric Oxide 14, 180–187.
Nicoletti, F., et al., 2011. Metabotropic glutamate receptors: from the workbench to the bedside. Neuropharmacology 60, 1017–1041.
Niswender, C.M., Conn, P.J., 2010. Metabotropic glutamate receptors: physiology, pharmacology, and disease. Annu Rev. Pharm. Toxicol. 50, 295–322.
Paoletti, P., 2011. Molecular basis of NMDA receptor functional diversity. Eur. J. Neurosci. 33, 1351–1365.
Paquet, M., Smith, Y., 2003. Group I metabotropic glutamate receptors in the monkey striatum: subsynaptic association with glutamatergic and dopaminergic afferents. J. Neurosci. 23, 7659–7669.
Picconi, B., et al., 2012. Synaptic dysfunction in Parkinson's disease. Adv. Exp. Med Biol. 970, 553–572.
Qiu, M.H., et al., 2014. Neuronal activity (c-Fos) delineating interactions of the cerebral cortex and basal ganglia. Front Neuroanat. 8, 13.
Quintero, J.E., et al., 2011. Methodology for rapid measures of glutamate release in rat brain slices using ceramic-based microelectrode arrays: basic characterization and drug pharmacology. Brain Res. 1401, 1–9.
Rascol, O., et al., 2014. Use of metabotropic glutamate 5-receptor antagonists for treatment of levodopa-induced dyskinesias. Park. Relat. Disord. 20, 947–956.
Scofield, M.D., Kalivas, P.W., 2014. Astrocytic dysfunction and addiction: consequences of impaired glutamate homeostasis. Neuroscientist 20, 610–622.
Shan, L., et al., 2015. L-Dopa induced dyskinesias in Parkinsonian mice: disease severity or l-Dopa history. Brain Res. 1618, 261–269.
Smith, P.J.S., et al., 2007. Principles, Development and Applications of Self-Referencing Electrochemical Microelectrodes to the Determination of Fluxes at Cell Membranes. In: Michael, A.C., Borland, L.M. (Eds.), Electrochemical Methods for Neuroscience. CRC Press, Boca Raton, FL.
Sofroniew, M.V., 2009. Molecular dissection of reactive astrogliosis and glial scar formation. Trends Neurosci. 32, 638–647.
Tata, D.A., Yamamoto, B.K., 2008. Chronic stress enhances methamphetamine-induced extracellular glutamate and excitotoxicity in the rat striatum. Synapse 62, 325–336.
Williams, S.M., et al., 2005. Glial glutamate transporter expression patterns in brains from multiple mammalian species. Glia 49, 520–541.